Comparative Transcriptome Analysis of Hypocotyls During the Developmental Transition of C_3 cotyledons to C_4 Leaves in *Halimocnemis mollissima*: Exploring Root-Shoot Signalings Involved in the Establishing of C_4 traits

Mahdis Zolfaghar[1], Mohammad Reza Ghaffari[*2], Ali Mohammad Banaei-Moghaddam[*1]

[1] Laboratory of Genomics and Epigenomics (LGE), Institute of Biochemistry and Biophysics, University of Tehran, Tehran, Iran

[2] Systems Biology Department, Agricultural Biotechnology Research Institute of Iran (ABRII), Agricultural Research, Education, and Extension Organization (AREEO), Karaj, Iran

[*] Correspondence:

Mohammad Reza Ghaffari

ghaffari@abrii.ac.ir (M.R.G)

Ali Mohammad Banaei-Moghaddam

am_banaei@ut.ac.ir (A.M.B-M)

Keywords: C_4 photosynthesis, NAD-ME subtype, *Halimocnemis mollissima*, long-distance signaling, RNA sequencing, hypocotyls

Abstract

Identification of various aspects of C_4 photosynthesis regulation is essential for introducing the C_4 pathway into C_3 crops. Species with dual photosynthesis in their life cycle are

interesting models to study such regulatory mechanisms through comparative analysis due to the lack of phylogenetic noises. Accordingly, the present research used *Halimocnemis mollissima*, which belonged to the Caroxyleae tribe, with C_3 (in cotyledons) and NAD-ME subtype of C_4 photosynthesis (in first leaves onwards) in its annual life cycle. We focused on exploring long-distance signaling pathways that are probably implicated in the shoot-root coordination associated with the manifestation of the C_4 traits, including efficient resource usage by comparing the mRNA content of hypocotyls before and after C_4 first leaves formation. As most likely part of the gene expression changes in hypocotyls observed in our study reflect those involved in the development of hypocotyls, we tried to exclude them by comparing our data with differentially expressed genes (DEGs) that had previously been identified in developing hypocotyls of flax and hemp. Our analyses revealed that several mobile regulators were differentially expressed in two developmentally different hypocotyls of *H. mollissima*, which belong to various transcription factors (TFs), phytohormones metabolism, and signaling peptides. Moreover, several up-regulated TFs in hypocotyls after establishing the C_4 first leaves were stress-responsive. Our results provide insights into the necessity of above- and under-ground tissue communication during the developmental transition of photosynthesis strategy in this species to manifest functional C_4 traits, especially nitrogen and water use efficiency and drought resistance.

INTRODUCTION

As an adaptation to the hot and dry environment, C_4 photosynthesis is a carbon concentration mechanism that reduces the counteracting photorespiration by suppressing the oxygenase activity of carboxylating enzyme RuBisCO (Ribulose-1,5-bisphosphate carboxylase/oxygenase). The leaves of C_4 plants have a unique structure called Kranz anatomy, enabling them to spatially separate two phases of photosynthesis into the mesophyll and bundle sheath cells. Generally, in the C_4 pathway, the carbon fixation begins in the

mesophyll, where carbon dioxide is converted into bicarbonate and then to four-carbon organic acids. The produced C_4 compound is then transported to the bundle sheath and decarboxylated to release the CO_2 at the site of RuBisCO for assimilation (Sage, 2004; Gowik and Westhoff, 2011). The Kranz anatomy precedes and facilitates evolving C_4 biochemistry, such as compartmentation and increasing the activities of key C_4 enzymes (McKown and Dengler, 2007). NADP-ME and NAD-ME are two main biochemical subtypes of the C_4 pathway based on the primary decarboxylating enzymes (Rao and Dixon, 2016).

The C_4 photosynthesis has evolved from C_3 progenitors in more than 60 independent lineages of angiosperms as a striking instance of convergent evolution (Slewinski, 2013). The polyphyletic origin of C_4 syndrome implies that the evolvement of C_4 from C_3 ancestors is not as genetically complicated as inferred from its associated anatomical and biochemical features. It is suggested that the pre-existing C_3 gene regulatory networks are recruited in the evolved C_4 pathway with relatively few modifications (Hibberd and Covshoff, 2010; Reyna-Llorens and Hibberd, 2017).

Besides the initial efforts that targeted the identification of genes encoding C_4 enzymes, recently, there have been several high throughput comparative studies aimed at identifying genetic architecture and regulation of setting up the C_4 metabolism (Gowik *et al.*, 2011; Wang, Vlad and Langdale, 2016; Cui, 2021). Such studies either have compared transcriptome profiles of C_3 and C_4 tissues belonging to the same (C_3 and C_4 *Flaveria*) (Gowik *et al.*, 2011) or different (C_3 rice and C_4 maize) (Wang *et al.*, 2014) species. Most of the omic analyses on C_4 photosynthesis have been performed in the C_4 plants that belong to NADP-ME subtypes (Gowik *et al.*, 2011; Lauterbach *et al.*, 2017), while investigation of both biochemical subtypes is essential to understand the nature and commonality of regulatory features of C_4 syndrome. More recently, species with two photosynthetic mechanisms in their life cycle have been noticed and investigated, such as *Haloxylon*

ammodendron (Y. Li *et al.*, 2015) and *Salsola soda* (Lauterbach, Billakurthi, *et al.*, 2017). Species with the developmental transition from a C_3 to C_4 pathway provided an excellent model for studying the molecular regulatory mechanisms underlying the coordination of roots and modified shoots during the C_3 to C_4 conversion, eliminating the disadvantages of associated phylogenetic noises with the former studied models. In these species, unlike the C_3 pathway in cotyledons, which coincide with moderate temperature, the C_4 pathway outperforms at higher light and temperature conditions concurrent with the formation of the first leaf stage onwards (Lauterbach, Billakurthi, *et al.*, 2017). Nevertheless, the dual photosynthesis performing species in these two studies belong to the Salsoleae tribe and perform the NADP-ME subtype of C_4 photosynthesis. Therefore, we used *H. mollissima* as a model to address this question and define the genes and regulatory pathways potentially associated with first leave ontogeny and the C_4 traits. *H. mollissima* belongs to the Caroxyleae tribe, which performs both C_3 (in cotyledons) and C_4 photosynthesis (NAD-ME subtype, in first leaves onwards) in its life cycle (Akhani *et al.*, 2009).

In addition to Kranz anatomy, the higher usage efficiency of resources such as nitrogen, water, and radiation is a universal feature of C_4 plants (Vogan and Sage, 2011; Fatima *et al.*, 2018). Generally, nitrogen and water are uptaken by roots based on their status and necessity in the shoots. Diverse long-distance signaling molecules such as phytohormones, signaling peptides, and TFs accomplish the shoot-root communication, which is essential for coordinating the growth and development of plants (Ko and Helariutta, 2017). Similarly, the onset of the C_4 pathway in leaves, followed by increased photosynthesis rate and more efficient use of resources, requires coordination between roots and the modified shoots via signaling molecules. In this regard, interspecies grafting experiments between C_3 *Flaveria robusta* and C_4 *Flaveria bidentis* indicated that the root preliminary controls sulfur allocation between roots and shoots and sulfur homeostasis in C_4 *Flaveria* (Gerlich *et al.*, 2018). The

nature and mechanism of distant signaling molecules act in C_4 plants to coordinate the above- and under-ground tissues to maintain their homeostasis and establish C_4 features, including Kranz anatomy, nitrogen, and water use efficiency, remains largely obscure and has hampered the long-standing goal of engineering C_4 metabolism into the C_3 crops. A comprehensive understanding of their underlying molecular genetics is crucial to overcoming the developmental barriers of introducing C_4 into the C_3 crop (Sage, 2004).

Many shoot-to-root or vice versa signals move through vasculature systems or cell-by-cell via stems or stem-like tissue, hypocotyls, based on the principle of hypocotyl micrografting (Bartusch and Melnyk, 2020). Moreover, the phloem comprises several mobile developmental signals (mRNAs, proteins, peptides, e.g.), which can play an interplay role in the different stages of development and growth (Koenig and Hoffmann-Benning, 2020). Accordingly, we generated transcriptome profiles of hypocotyls before and after forming the C_4 first leaves by RNA sequencing to explore possible mobile signals moving between shoots and roots regulating the establishment of functional C_4 traits while they would be in control of the developmental photosynthetic transition. Our finding reconfirmed the NAD-ME subtype of C_4 photosynthesis in the first leaves of *H. mollissima* as a higher abundance of NAD malic enzyme (NAD-ME) than NADP malic enzyme (NADP-ME) was observed. Besides, genes associated with several phytohormone metabolisms, TFs, and signal peptides were differentially expressed in hypocotyls before and after the formation of C_4 first leaves. Comparing these differentially expressed genes with identified genes associated with hypocotyl development in different species (Roach and Deyholos, 2008, Behr *et al.*, 2018)) showed that parts of these genes are likely associated with hypocotyl development.

Nevertheless, our results indicated that some of these genes show homology to known shoot to root and vice versa signals and their receptors that are possibly implicated in establishing

unique C_4 traits, especially in the efficient consumption of resources such as nitrogen and water.

MATERIALS AND METHODS

Plant Cultivation and Sampling

Seeds of *H. mollissima* were collected at Mahdasht, Karaj, Iran (35°43'35.4"N; 50°44'04.5"E) in November 2019. The seeds were deposited at 4°C. First, the hard seed coats were removed, disinfected with ethanol 75%, and then washed with water. The seedlings were grown on the wet sterilized filter papers in the Petri dishes. After root formation, in 3 days, the seedlings were transferred into the plastic pots (5 cm in diameter, 7 cm in height) filled by the sands, perlite, and compost. The *H. mollissima* were grown in a greenhouse at the Institute of Biochemistry and Biophysics, University of Tehran, at temperature 25-30°C with supplementary illumination of ~200 μmol m^{-2} s^{-1} 16/8-hours light/dark cycle.

For sampling, two series of *H. mollissima* were cultivated. We harvested expanded cotyledons and hypocotyls (hypocotyl A) in the first series before forming the first leaves. In the second series, we sampled cotyledons, hypocotyls (hypocotyl B), and first leaves after forming the first leaves (Figure 1). The tissues of interest were sampled in January and February 2020 between 11:00 and 13:00 and immediately placed in the liquid nitrogen, then stored in -80°C. Two biological replicates were examined, each containing pooled tissue from 5 independent plants.

RNA Extraction and Sequencing

The guanidine/ phenol-based method (Chomczynski and Sacchi, 1987) was used to isolate total RNA from 100-150 mg of the homogenized samples. The quality, quantity, and integrity of isolated RNA were checked by Agarose gel electrophoresis, Nanodrop (Thermo Fisher

Scientific), and Agilent Bioanalyzer 2100 system (Agilent Technologies Co. Ltd., Beijing, China), respectively. High-quality RNA (RIN value more than 5.2) was used for cDNA preparation and sequencing by Illumina Hiseq 2500 platform at the Novogene Bioinformatics Institute (Beijing, China). One hundred fifty bp paired-end reads were obtained, and their adapter-contained and low quality (Qscore< = 5) base-contained were removed.

De novo Assembly and Functional Annotation

Raw reads were evaluated for quality by FastQC tool (http://www.bioinformatics.babraham.ac.uk/projects/fastqc/). Due to removing adapters and low-quality reads by the Novogene Bioinformatics Institute, there was no need for trimming. The high-quality reads were assembled by Trinity v2.4.0 (Grabherr *et al.*, 2011) using default settings. To evaluate the Trinity results, N50 and the total assembly length were checked.

First, probable open reading frames (ORF) were predicted using the Transdecoder tool (Haas and Papanicolaou, 2016) with a minimum length of 100 amino acids. To obtain Gene Ontology (GO) terms of the transcripts, Blast2GO software was used with $1e^3$ as an e-value cut-off to perform BlastX against a non-redundant protein database. Moreover, the online KEGG Automatic Annotation Server (KAAS) (http://www.genome.jp/kegg/kaas) and Mapman V4.0 (https://www.plabipd.de/portal/mercator4) (Schwacke *et al.*, 2019) were used for pathway analysis (p-value $\leq$ 0.05). Also, the Arabidopsis TAIR locus IDs were assigned to each transcript during Mapman analysis (https://www.plabipd.de/portal/web/guest/mercator-sequence-annotation) (Lohse *et al.*, 2014).

Determination of Genes with Different Expression

RSEM tool (http://deweylab.biostat.wisc.edu/RSEM) (Li and Dewey, 2011) was used to estimate the abundance of the transcripts for each sample. The high-quality raw reads were

separately mapped back onto the assembled transcripts using the Bowtie 2.0. Differential expression analysis was performed by edgeR (Robinson, McCarthy and Smyth, 2010) in R after normalization using the trimmed mean of M-values (TMM) method in edgeR. Statistical tests for the pairwise comparisons were Benjamini-Hochberg correction FDR ≤ 0.05, $\log_2$FC ≥ 1.5, ≤ -1.5 to set a significant threshold for the determination of DEGs. Principal component analysis (PCA) with $\log_2$ transformed read count (Transcript Per Million TPM) was performed in RStudio to visualize the expression pattern of the samples. Furthermore, hierarchical clustering of the transcript abundance of selected known C_4 proteins using Pearson correlation, average linkage method was performed (http://www.heatmapper.ca/expression/).

The differentially expressed genes which are associated to the hypocotyl development of *H. mollissima* excluded from further analysis by comparing them with differentially expressed genes involved in the hypocotyl development in other plants (Roach and Deyholos, 2008, Behr *et al.*, 2018) through Venn diagram (https://bioinformatics.psb.ugent.be/webtools/Venn/).

UpSet Plot and Functional Analysis

Shared and unique DEGs in the three pairwise comparisons were indicated using the UpSet plot (https://gehlenborglab.shinyapps.io/upsetr/).

Pathways in each developmental tissue of interest were explored using the percentage of total transcripts (normalized to Transcript Per Million (TPM)) of each particular bincode in Mapman V4.0.

According to the further emphasis of this study on the survey of probable long-distance signaling, gene enrichment analysis was conducted by PageMan software (Usadel *et al.*, 2006) through Fisher's exact test followed by the Benjamini-Hochberg correction to identify

significant differences of Mapman bins among the different samples. Moreover, Mapman V3.6.0RC1 was used to visualize selected differentially expressed genes encoding phytohormone synthesizing and degrading enzymes, transporter ("Phytohormone action bin" and "Solute transporter"), and also genes related to different signal transduction pathways ("Multi-process regulation. Calcium-dependent signalling", "Protein modification. Protein kinase" and "Redox hemoestasis" bins).

Identification of TFs and Prediction of Cis-acting elements in the Promoter of Predicted Mobile TFs

To predict differentially expressed TFs between hypocotyl before and after the formation of first leaves, the homology of related amino acid sequences against the plant TFs database (PlantTFDB V5.0, http://planttfdb.gao-lab.org/prediction.php) was implemented. Afterward, we predicted TFs, which are shown to have mobile mRNA based on the information about the genes with "cell-to-cell mobile mRNA" in The Arabidopsis Information Resource (TAIR) database.

Since the *H. mollissima* genome is not yet available, the promoter region of the orthologs of predicted mobile TFs in Arabidopsis (as a well-known model) was obtained from the Arabidopsis Gene Regulatory Information Server (AGRIS) database (https://agris-knowledgebase.org/AtcisDB/), and their cis-acting were predicted using PlantCARE (http://bioinformatics.psb.ugent.be/webtools/plantcare/html/).

RESULTS

Processing of Raw Reads and Statistics of De novo Assembly

According to our aim, mRNA of three different tissues, including hypocotyls before the formation of the first leaves (hypocotyl A), hypocotyls after the formation of first leaves

(hypocotyl B), and the first leaves (FL), were sequenced. The quality of reads was checked, and based on fastQC results (Phred score= 36), all reads had high quality (Supplementary Table S1(A)) without the need for further trimming. Raw data is available in the ? database under accession number ? (Supplementary Table S2). PCA analysis (Figure 2), where the first principal component contained 69.57% and the second principal component had 21.52% of the variance, demonstrated that the analyzed tissues have a distinct expression pattern. Nevertheless, the replicates' expression data were similar and grouped. As expected, the same tissues (hypocotyl A and hypocotyl B) had more similar expression patterns than the first leave.

Transcriptome *de novo* assembly was conducted by Trinity assembler, and the basic quality assessment was obtained by Trinitystat.pl (Supplementary Table S1 (B)).

Determination of Active Functional Pathways in each tissue

To evaluate how the transcriptome as whole changes during the developmental transition of photosynthesis strategy, the functional classes of each tissue transcriptome were determined as the percentage of all transcripts (normalized to Transcript Per Million (TPM)) assigned to each Mapman bincodes (Figure 3, supplementary table S3). MapMan analysis showed "Not assigned, annotated" and "Not assigned, not annotated" with 19.41 and 45.86% of all transcripts being the most statistically significant functional gene categories in each sample. As expected, the "Photosynthesis" bin was the third-highest abundant functional class in the first leaves (15.44%), while this amount was significantly lower in the hypocotyl A (3.25%) and B (2.47%). Besides, the abundance of transcripts encoding the C_4-related proteins was compared between FL and hypocotyls (Figure 4). As expected, out of 16 transcripts associated with known C_4 proteins, 14 transcripts, including Beta-carbonic anhydrase (BCA3), PEP carboxylase1 (PEPC1), pyruvate orthophosphate dikinase (PPdK), aspartate

aminotransferase (Asp-AT), alanine aminotransferase (Ala-AT), NAD-dependent malic enzyme (NAD-ME), NADP-dependent malic enzyme (NADP-ME), Triosephosphate translocator (TPT), Pyrophosphatase (PPase6), pyruvate orthophosphate dikinase related protein1 (PPdK-RP1), PEP/phosphate translocator (PPT2), Bile acid:sodium symporter family protein (BASS4), Bile acid:sodium symporter family protein (BASS2), Adenosine monophosphate kinase (AMK2) were more abundant in FLs than hypocotyls (Figure 4) (Supplementary Table S4). NAD-ME is more abundant than NADP-ME in FLs.

"Protein biosynthesis" and "Protein homeostasis" were the third- and fourth-highest abundant functional categories in hypocotyl A (4.68 and 3.96%, respectively) and B (4.67 and 4%, respectively) (Figure 3). "RNA biosynthesis" (1.92-2.34%) and "solute transport" (1.87-2.09%) were also abundant in all three samples (Supplementary Table S3). Although generally, most of the functional categories' abundance is similar between the two developmentally different hypocotyls of A and B, however, "RNA biosynthesis" (2.04 and 2.34 %, respectively) and "Phytohormone action" (1.2and 1.31%, respectively) classes are somewhat more abundant in the hypocotyl B than A.

Pairwise comparison of samples revealed 8422, 3095, and 11888 DEGs for hypocotyl B vs. hypocotyl A, hypocotyl A vs. FL, and hypocotyl B vs. FL, respectively (Supplementary Table S5). The number of unique and shared DEGs between each binary comparison of samples is shown in Figure 5. In general, 1032 (VI and VII sections in figure 5) shared DEGs between hypocotyl A vs. FL and hypocotyl B vs. FL are probably associated with the hypocotyl-specific genes. Most of these genes were included in the "not assigned", "RNA and protein biosynthesis, processing and hemostasis" bins. Most of the DEGs are unique in the binary comparisons (a total of 9966 (I, III, and V sections in figure 5) DEGs).

Focusing on our main aim to identify possible signaling pathways involved in the developmental transition of C_3 to C_4, pathways enrichment analysis was conducted for DEGs in hypocotyl B vs. hypocotyl A comparison. Out of 8422 DEGs, several pathways were enriched after overrepresentation analysis (Figure 6). Transcripts related to the "Protein biosynthesis" bin and "Protein homeostasis. Ubiquitin-proteasome system" were up-regulatedly overrepresented in hypocotyl B compared to hypocotyl A.

Next, to explore possible long-distance regulators, we focus on the various regulatory mechanisms by further analyzing differentially expressed genes in the two developmentally different hypocotyls. To differentiate the genes controlling the developmental transition of photosynthesis strategy from the genes involved in hypocotyl development, we compared them (based on the assigned Arabidopsis IDs) with the identified associated genes with hypocotyls development (Roach and Deyholos, 2008; Behr *et al.*, 2018). We then focused on the unique genes which do not overlap with related developmental genes (Supplementary Figure 1, Supplementary Table S6).

The Differentially Expressed Genes associated with Classical Phytohormones Metabolism

Mapping the DEGs of hypocotyl B Vs. hypocotyl A to the cell signaling pathway genes in Mapman V3.6.0RC1 (Figure 7, Supplementary Table S7) indicated several genes involved in the biosynthesis, degradation, transport, and signal transduction of plant hormones (Phytohormone bin in Mapman) are up- or down-regulated in hypocotyl after the establishment of C_4 photosynthesis in the first leaves.

Several transcripts encode auxin transporters, such as PIN-FORMED (PIN) (PIN2; At5g57090), and ATP-binding cassette-B (ABCB) auxin transporter (ABCB19; At3g28860), which are located on the plasma membrane and involved in long-distance auxin signaling

were less abundant in hypocotyl B compared to hypocotyl A. Besides, some auxin-responsive genes like NITRATE TRANSPORTER 1 (NRT1; AT1G12110), an auxin-responsive transporter, were down-regulated in hypocotyl B. Moreover, the corresponding transcript of flavin-dependent monooxygenase (YUCCA) involved in auxin biosynthesis was down-regulated in hypocotyl B after C_4 establishment. In contrast, transcripts of some other transporters belonging to PIN-Like transporters (PILS), distributed in the intracellular compartments and mediate intracellular auxin homeostasis, were more abundant in hypocotyl B. Besides, transcripts assigned to AUX/ IAA (AT5G43700, AT3G04730, AT4G29080) and ARF7/ARF19 (AT1G19220) auxin signal transduction genes were up-regulatedly enriched in hypocotyl B. Altogether, it seems the biosynthesis and long-distance transport of auxin are reduced in hypocotyls after the formation of the first leaves.

Almost all transcripts associated with different cytokinin pathways bin were up-regulated in hypocotyl B (Figure 7). Cytokinin-specific phosphoribohydrolase, from the LONELY GUY (LOG) family, is an enzyme in the cytokinin biosynthesis pathway (Kurakawa *et al.*, 2007) which its corresponding transcripts (AT5G06300) were up-regulated in the hypocotyl B. This enzyme directly catalyzes inactive cytokinin's conversion to the biologically active free-base forms in one step. Moreover, transcripts associated with cytokinin dehydrogenases (AT2G41510, AT3G63440, AT1G75450) and UDP-glycosyltransferases (AT2G15490), which are implicated in the degradation and conjugation of cytokinin, were more expressed in the hypocotyl B. Type-B ARABIDOPSIS RESPONSE REGULATOR (ARR) is the positive regulator of cytokinin signaling (Argyros *et al.*, 2008) and type-A ARR is the negative regulator of cytokinin signaling (To *et al.*, 2004) which their corresponding transcripts (AT1G67710 and AT3G57040) were up- and down- regulated in the hypocotyl B, respectively. Also, transcripts of ENT (EQUILIBRATIVE NUCLEOTIDE TRANSPORTER

1) (at1g70330), importers to take up apoplastic nucleosides of cytokinins, were more expressed in the hypocotyl B.

Several hormone transporters were more expressed in hypocotyl B (Figure 7, Supplementary Table S7), such as ABCG30, ABCG40, LHT1 (LYSINE-HISTIDINE TRANSPORTER). These hormone transporters take part in the long-range hormone transport and distribution via the vascular system (Lacombe and Achard, 2016). ABCG30 (AT4G15230) and ABCG40 (AT1G15520) play roles in the abscisic acid influx and efflux, respectively (Kang *et al.*, 2015). Moreover, LHT1 (at5g40780) is an amino acid carrier associated with the transport of ethylene precursor, 1-aminocyclopropane-1-carboxylic acid (ACC). NPF3.1 (Nitrate transport1/Peptide transporter family) (at1g68570) is down-regulated in hypocotyl B. It is a multihormone transporter involved in the GA/ABA antagonism (Hirner *et al.*, 2006). Besides, all DEGs associated with brassinosteroids were down-regulated.

The Differentially Expressed Signaling Peptides

Cysteine-rich peptides (CRP) and non-cysteine-rich peptides (NCRP) represent the two main classes of signaling peptides in plants (Marshall, Costa and Gutierrez-Marcos, 2011; Okamoto, Tabata and Matsubayashi, 2016). Overrepresentation analysis of differentially expressed genes in hypocotyls before and after the formation of the first leaves revealed that, in contrast to the CRP classes of plant peptides, transcripts related to NCRP did not show enrichment in hypocotyls after the formation of the first leaves (Figure 6). Transcript abundance of different groups of these classes, based on Mapman bins, was then compared between analyzed tissues and showed a complex pattern of up and down-regulation of transcripts encoding different groups of signaling peptides (Figure 8). In general, transcripts belonging to different groups of the CRP categories were less abundant in hypocotyls after the establishment of C_4 photosynthesis in the first leaves (Figure 8 (A)). In this regard,

transcripts assigned to the several GASA group members, including GASA1 (at1g74670), GASA8 (AT2G39540), GASA13 (AT3G10185), GASA14 (AT5G14920), and GASA 10 (AT5G59845) as well as RALF signaling peptides like RALF33 (AT4G15800) and its receptor CrRLK1L were down-regulated in hypocotyl after C_4 manifestation. The transcripts encoding some groups of peptides belong to the NCRP classes, including plant natriuretic peptide (PNP), CLAVATA3-EMBRYO-SURROUNDING REGION (CLE), Casparian strip integrity factor (CIF), PAMP-INDUCED SECRETED PEPTIDE (PIP), Phytosulfokine (PSK) are more expressed in the hypocotyl after the formation of first leaves (Figure 7, Figure 8 (B)). However, transcripts that are assigned to the receptor of C-terminally Encoded Peptides (CEP) like CEPR2 (AT1G72180) act in the nitrogen uptake signaling and Root meristem growth factor (RGF), were down-regulated in hypocotyl after the first leaves formation.

The Differentially Expressed Genes Taken Part in Various Signal Transduction Pathways

The binding of the ligands to their receptors at the surface of the cells triggers intracellular reaction cascades to amplify the input signals, which eventually leads to the alteration of gene expression in various pathways. In this study, transcripts encoding different genes involved in the transduction pathways were differentially regulated in the hypocotyls after the formation of the first leaves (Figure 7). Transcripts of varying protein kinase families, which are essential components implicated in a multitude of cell signaling, were more abundant in hypocotyl after the formation of the first leaves. In this regard, all DEGs belonged to the genes associated with casein kinase (CK) and sterility (STE) protein kinase superfamilies. Most genes belonged to the AGC (PKA-PKG-PKC), and CMGC (Cyclin-dependent kinases, Mitogen-activated protein kinases (MAPK), Glycogen synthase kinases, and Cyclin-dependent like kinases) superfamilies were more expressed in hypocotyl B. Moreover, the

greatest numbers of transcripts associated with receptor-like cytoplasmic protein kinases (RLCKs) were more transcribed in hypocotyl B.

Redox signaling is another transduction pathway in which genes involved in the ascorbate-, glutathione- and thiol-based redox regulation are more enriched in the hypocotyl after the formation of first leaves. Likewise, calmodulin-like proteins (CMLs) are the largest class of Ca^{2+} sensors in plants during Ca^{2+} signaling, and were up-regulately expressed in hypocotyl after the formation of first leaves.

The Differentially Expressed TFs

According to PlantTFDB V5.0, 290 out of 9640 ORFs from differentially expressed transcripts between hypocotyl before and after the formation of first leaves, annotated as different TF families with the best fit in *A. thaliana* locus IDs (Supplementary Table S8). The mRNA levels of 71 and 219 of these TFs were down- and up-regulated, respectively, in hypocotyl after the formation of the first leaves. In this comparison, C2H2, bHLH, and NAC families had a larger number of differentially regulated transcripts. Almost all transcripts belonged to C2H2, C3H, GRAS, MYB, TCP, Trihelix, NF-Y, and WRKY TFs had more expression in hypocotyl after the formation of first leaves. SHORT ROOT (SHR) (AT4G37650), a member of the GRAS family and ELONGATED HYPOCOTYL 5 (HY5) (AT5G11260, AT3G17609), a member of the basic leucine zipper (bZIP) family, were up-regulated in hypocotyl after the formation of the first leaves. Notably, both SHR and HY5 are shown to have mobility and could affect the expression of other genes (Dolan, 2001; Chen *et al.*, 2016).

Among 290 differentially expressed transcripts that were annotated as TFs based on PlantTFDB, 12 of them had orthologous with cell-to-cell mobile mRNA according to the TAIR database (Table 1). Eight of these TFs were more abundant in hypocotyl after the

formation of the first leaves, including SCL1 (GRAS family, AT1G21450), HAT22 (HD-ZIP family, AT4G37790), HSFA1E (HSF family, AT3G02990), CDC5 (MYB_related, AT1G09770), MYBH (MYB_related family, AT5G47390), NAC053 (NAC family, AT3G10500), NAP (NAC family, AT1G69490) and ATWRKY40 (WRKY family, AT1G808$_4$0).

To predict if specific cis-regulatory elements are overrepresented in the regulatory region of the candidate mobile TFs with differentially expression levels in hypocotyls, PlantCARE (Lescot *et al.*, 2002) was used to analyze the upstream promoter elements of the Arabidopsis orthologs of these transcripts. The analyses showed that Arabidopsis orthologs of differentially regulated mobile TFs carry several different cis-elements responsive to the phytohormones and environmental stimuli such as light and temperature. Box 4 (part of a conserved DNA module involved in light responsiveness), AE-box (part of a module for light response), G-Box (cis-acting regulatory element involved in light responsiveness), and GT1-motif (light-responsive element) were more common in the upstream of the mobile TFs (Supplementary Table S9). Besides, the ABA-responsive element (ABRE) was predicted in the promoter of BOA, SCL1, HAT22, MYBH, NAC053, ATAF1, NAP, and WRKY40 TFs. Other motifs related to stress responses, including MYB binding site involved in drought-inducibility (MBS), cis-acting element involved in defense and stress responsiveness (TC-rich repeat), and cis-acting regulatory element involved in the MeJA-responsiveness (CGTCA-motif and TGACG-motif), were predicted to be present in the upstream region of the orthologs of mobile TFs genes modulated after the formation of the first leaves. Notably, three out of four downregulated mobile TFs in hypocotyls after forming first leaves had TGA-element, an auxin-responsive element. In contrast, only one out of eight up-regulated mobile TFs had such elements in its regulatory region.

DISCUSSION

Species with Switching Mechanisms are Valuable Models to study C_4 photosynthesis

We investigated the transcriptome profile of *H. mollissima* hypocotyls alongside its first leave as a model to search for components of long-distance signaling pathways involved in the developmental transition of C_3 to C_4 photosynthesis. *H. mollissima* belongs to *the* Caroxyleae tribe. It is already shown that this species is a switching chenopod and has two photosynthetic mechanisms in its annual life cycle; C_3 in cotyledons and NAD-ME subtype of C_4 in the first leaves onwards (Akhani *et al.*, 2009). In natural environments, several species in the subfamily Salsoloideae (Caroxyleae and Salsoleae tribes) and fewer in Suadedoideae have switching mechanisms (Rudov *et al.*, 2020). These species inhabit mainly the area with continental climates. Thus, their germination coincides mainly with low-temperature conditions that would possibly favor C_3 photosynthesis in the cotyledons. As these species grow and the temperature rises, C_4 photosynthesis is encouraged in the leaves (Rudov *et al.*, 2020). The species with the switching mechanism can be an appropriate model to explore the C_4 pathway and its regulatory mechanisms due to the lack of phylogenetic noises and interspecies differences. In this regard, transcriptome analysis of *Haloxylon ammodendron* (Y. Li *et al.*, 2015) and *Salsola soda* (Lauterbach, Billakurthi, *et al.*, 2017) have previously investigated which belong to the *Salsoleae* tribe and perform NADP-ME subtype of C_4 photosynthesis in their first leave onwards. These studies compared transcriptome profiles of tissues performing C_3 and C_4 photosynthesis at different developmental stages, including cotyledons (C_3) and assimilating shoots (C_4). Their results mainly revealed differentially expressed C_4 pathway genes, between C_3 cotyledons and C_4 true leaves, and less attention was paid to the differences in regulatory pathways. Our research investigated potential shoot-root communications during the C_3 to NAD-ME subtype of C_4 transition. Therefore, it focused on the differentially expressed genes in hypocotyls before and after the C_4 first leave's formation.

Novel Consistent Data Provided by *De novo* Assembly of *H. mollissima* transcriptomes

Most of the transcriptome data analyses of other publications in the field of C_4 photosynthesis, with a few exceptions, have used a reference-based approach to annotate their data using the Arabidopsis data (Gowik and Westhoff, 2011; Lauterbach, Billakurthi, *et al.*, 2017; Lauterbach, Schmidt, *et al.*, 2017; Siadjeu, Lauterbach and Kadereit, 2021). As a non-model species in the Caroxyleae tribe whose genome is not sequenced, we used RNA-seq to de novo assemble and characterize the *H. mollissima* hypocotyls and first leaves transcriptome. Principal component analysis of the read counts separated the samples based on the tissue type and indicated the consistency and validation of our normalized data. Analysis of functional classes of annotated genes (Figure 3) showed overall active pathways among the tissues of interest.

Altogether, PCA and analysis of functional classes of annotated genes confirm the sequencing data's reasonable and comparable relationship. As expected, based on the functional annotation, the NAD-ME subtype of the C_4 photosynthesis pathway was expressed in the first leaves. The photosynthesis reduced in hypocotyls after establishing the photosynthetic leaves. Hence, it can be concluded that hypocotyl A has more photosynthetic activity than hypocotyl B. Besides, the formation of first leaves leads to an increase in translation processes in the hypocotyls to act in different pathways. Likewise, many transcripts of the ubiquitin-proteasome system were up-regulated in hypocotyls, a critical regulator of many plants signaling pathways to respond to internal and external cues (Sadanandom *et al.*, 2012).

Possible Regulatory Mechanisms Implicated in the Unique C_4 Features through Adjustment of Shoot and Root communication

Several regulatory systems with overlapping functions control the various developmental processes in plants. These regulatory systems include but are not limited to the phytohormones, signaling peptides, and complex network of TFs. Long-range regulators (Inter-tissue movement) are an essential part of these systems. As the mobile signals between the above- and under-ground tissues are transmitted through the stem or stem-like tissues, hypocotyls, we compared transcriptome profiles of hypocotyls during C_3 cotyledon to C_4 true leaves transition. Our comparative transcriptome analysis revealed that transcripts of genes encoding components of different phytohormones, signaling peptides, and TFs (Figure 7, Supplementary Table S7) were differentially expressed in hypocotyls after establishing the C_4 leaves. In addition, the transcript abundance of several transporters, receptors, and responsive genes of root- or leaf-derived signals were changed in hypocotyls during C_3 to C_4 transition, including PIN1, CEPR, and ARF7/ARF19. Thus, their up- or downregulation in hypocotyls during the transition of photosynthesis strategy likely reflected in the expression of signals in roots or leaves. It is noteworthy that a number of these regulators are most likely implicated in the normal development of hypocotyls. Therefore, to strengthen our DEGs of two developmentally different hypocotyls as C_4-related genes, we excluded the genes involved in the hypocotyl development based on the literature survey (Supplementary Fig. 1, Supplementary Table 6). For example, Mellisa J. Roach et al. (2008) (Roach and Deyholos, 2008) analyzed microarray data on developing hypocotyls in flax. Transcripts associated with cell-wall modification or primary-wall deposition were enriched during the hypocotyl development. Moreover, several TFs, hormone-related genes, calcium-signaling genes, and signal kinases related to the fiber development in hypocotyls were enriched. In another study, Marc Behr et. al (2018), investigated secondary growth and the molecular pathways of lignification at the transcriptional and proteomic levels during the development of the hemp hypocotyl (Behr *et al.*, 2018). We excluded the overlapped DEGs (based on their assigned

Arabidopsis IDs) of two developmental stages of *H. mollissima* hypocotyls and DEGs in the abovementioned studies to consider unique genes.

C_4 photosynthesis is performed in the leaves in response to the reduced atmospheric CO_2; hence, coordination between the root and the modified shoot seems necessary. The communication ways between above- and below-ground plant parts are very diverse and could be of physical (like propagating Ca^{2+} waves), chemical (like signaling peptides and hormones), or molecular (like proteins and RNA) nature, traveling from shoots to roots and vise versa (Shabala *et al.*, 2015). The potential of long-range movement for several differentially expressed regulators in hypocotyls has been already demonstrated, including auxin (Bellstaedt *et al.*, 2019), cytokinin, abscisic acid (Kiba *et al.*, 2011), various signaling peptides such as PNP (Morse, Pironcheva and Gehring, 2004), CLE and CEP and also their transporters and some TFs (Shabala *et al.*, 2015).

Nitrogen use efficiency: The Reduction of Shoot-to-Root nitrogen Status Signals after the Formation of the C_4 First Leaves

Nitrogen assimilation by roots can be controlled by a number of signals representing the nitrogen status in the shoots (Ruffel *et al.*, 2008; Forde, 2002), including phytohormones such as auxin and cytokinin (Kiba *et al.*, 2011).

It seems that some of the differentially expressed regulators in the comparison of hypocotyl B and hypocotyl A can play roles in the long-distance regulation of nitrogen uptake in the C_4 plants. Our results showed that several genes involved in the biosynthesis, transport, and biodegradation of phytohormones were differentially expressed in the hypocotyl after the formation of the first leaves. It has already been indicated that nitrogen availability in shoots interacts with some phytohormones (e.g., auxin and cytokinin) to regulate nitrogen acquisition by roots(Kiba *et al.*, 2011). In the present study, based on the up-regulation of

LOG1 and type-B ARRs, cytokinin active form and cytokinin signaling were increased. Indeed, it has been indicated that the type of shoot-derived cytokinin is a signal of nitrogen satiety in well-supplied nitrogen conditions, which suppress the nitrogen uptake by roots (Kiba *et al.*, 2011). Furthermore, our findings suggest that long-range cytokinin signaling can be a candidate pathway for controlling nitrogen uptake by the root in C_4 plants. Totally, there is no requirement to involve particular cytokinin transporters for this shoot-to-root movement through the phloem. However, ENTs are likely involved in this transfer (Liu, Zhao and Zhang, 2019) which was more expressed in hypocotyl B. Moreover, it is already reported that cytokinin interacting with another hormone signaling can affect hypocotyl length (Smets *et al.*, 2005).

Cell-to-cell auxin transporters, responsible for auxin's long-distance movement and an enzyme catalyzing the rate-limiting step in auxin biosynthesis, were down-regulated in hypocotyls B. In contrast, the intracellular auxin transporters that modulate the nuclear abundance of auxin by transporting auxin into the ER lumen (Sauer and Kleine-Vehn, 2019) were up-regulated. These findings imply that long-distance movement of auxin is decreased in hypocotyls after C_4 leaf formation. Due to the basipetal movement of auxin and its effect on the initiation of lateral roots, it has been long known as a shoot-to-root nitrogen signal (Forde, 2002; Fukaki and Tasaka, 2009). In maize, a C_4 crop, auxin concentration in the phloem exudates is decreased in high nitrate concentrations (Tian *et al.*, 2008).

In addition, the NRT1 transporter was down-regulated in hypocotyl after forming the first leaves. NRT1 has a significant role in the nitrogen uptake in roots affected by various signals derived from shoots. Alongside, As a multifunctional protein, it plays a role in various pathways, including auxin transport, nitrate signal transduction, integration of nutrient signal, and a regulatory role in plant-microbe interaction (Wang *et al.*, 2020). Besides its role as a dual-affinity transporter, NRT1 acts as a nitrate sensor and regulates the expression level of

other genes involved in nitrate transport (Sun and Zheng, 2015). The location of NRT1 is in roots, vascular cells, and shoots and has auxin-responsive activity. Therefore, its reduced expression is consistent with other findings in this study, implying a reduction of auxin content in the hypocotyls, either derived from leaves or the hypocotyl itself. It should be mentioned that there are few studies in the case of auxin involvement in the C_4 characteristics in which local auxin biosynthesis and transport are elevated in the C_4 leaves and are required to develop a high leaf vein (Huang *et al.*, 2017).

CEP is another mobile regulator mediating nitrogen assimilation in roots in the nitrogen deficiency condition, which has a shoot orientation from the roots. CEP receptor, like CEPR2, was down-regulated in hypocotyl B, most likely due to the efficient use of nitrogen by C_4 plants. Indeed, this receptor implicates nitrogen uptake signaling by enhancing the expression of NRT1 (Tabata *et al.*, 2014; Ohkubo *et al.*, 2017). Thus, its down-regulation in hypocotyls reflects the reduced effect of root-derived CEP signal after C_4 leave's formation.

Taken together, the observed gene expression changes indicate altered auxin and cytokinin metabolism and signaling, reducing CEP signaling in hypocotyls after emerging C_4 photosynthesis in the first leaves. The observations imply the fact that the nitrogen use efficiency is improved, and the total nitrogen requirement is decreased in C_4 plants (Jobe *et al.*, 2020).

Drought Resistance and Water use efficiency: Several Pathways involved in the High-Temperature Resistance after the Formation of the C_4 First Leaves

Through different mechanisms, C4 plants are more efficient producers than C3 in higher temperatures. One of them is that they prevent dehydration through stomatal closure. In our study, some influx and efflux of abscisic acid (ABCG30, ABCG40, and DTX) (Zhang *et al.*, 2014; Kang *et al.*, 2015) were up-regulated in C_4-associated hypocotyl. Accordingly, long-

distance shootward ABA transport can be proposed to increase during C_4 manifestation. Indeed, in C_4 plants, the stomata are closed, and therefore, CO_2 uptake and water loss through stomata were reduced. Some studies indicated that stomata of C_4 plants are more sensitive to intercellular CO_2 concentration (Ci) than C_3 (Huxman and Monson, 2003), and also, abscisic acid can increase such sensitivity (Dubbe, Farquhar and Raschke, 1978). Besides, the remote regulation of stomatal movement by root-derived abscisic acid is a central long-distance signal caused to stomatal closure in drought stress situations (Kuromori, Seo and Shinozaki, 2018). ABCG40 is a root-derived abscisic acid importer in shoots that play an essential role in the stomatal closure (Kang *et al.*, 2010). Accordingly, its up-regulation in hypocotyls likely implies more root-derived abscisic acid signals during manifestation of C_4 leaves. Likewise, stomatal closure, probably resulting from increased CO_2, is affected by long-distance ABA signals (Wilkinson and Davies, 2002). It is concluded from an investigation of *Pinus radiata* that foliage-derived ABA is a source of ABA signaling in the shoots for stomatal control (Sampaio Filho *et al.*, 2018). Moreover, induction of Kranz anatomy in amphibious *Eleocharis vivipara* indicates the significant role of abscisic acid and hormonal control in the manifestation of Kranz anatomy. However, the exact underlying mechanism remained elusive (Ueno, 1998).

Stress- and light-responsive differentially expressed mobile TFs in hypocotyls are possibly involved in the formation of C_4 unique features

Many of the TFs that are up-regulated in the hypocotyls after the formation of the first leaves are implicated in the regulatory networks controlling responses to the different plant development and growth conditions as well as the abiotic stresses. The appearance of C_4 leaves in *H. mollissima*, and other halophytes or xerohalophytes switching chenopods is accompanied by an increase in temperature (Rudov *et al.*, 2020). Transcriptome analysis of C_3 cotyledons and C_4 leaves in *Salsola soda* demonstrated that 55 and 32 TFs were increased

and decreased in C_4 leaves compared to C_3 cotyledons, respectively (Lauterbach, Billakurthi, *et al.*, 2017). Not surprisingly, a greater number of the up-regulated TFs in our study were stress-responsive, including NAC (Shao, Wang and Tang, 2015), WRKY (Wang *et al.*, 2018), and NF-Y (Zhao *et al.*, 2017).

Among differentially expressed TFs in hypocotyls before and after the formation of the C_4 first leaves, SHR and HY5 TFs are noteworthy to consider since they are shown to be mobile (Dolan, 2001; Chen *et al.*, 2016). SHR is implicated in modulating endodermis (known as bundle-sheath) differentiation in the leaves. It has been reported that SHR plays a role in the Kranz anatomy formation in maize (Slewinski *et al.*, 2012). Moreover, Christian Siadjeu, *et al.* (Siadjeu, Lauterbach and Kadereit, 2021) compared transcriptome data of C_3, C_2, and C_4 species from *Camphorosmeae*. Based on cluster analysis, BBX15, SHR, SCZ, and LBD41are more expressed and co-regulated in the C_4 than C_3 species. Interestingly, out of 38 differentially expressed Arabidopsis orthologous TFs in the comparative transcriptomic analysis between Kranz (foliar leaf blade) and non-Kranz (husk leaf sheath) maize leaves, four TFs were identified in the present study to express more in hypocotyl after C_4 leave's formation; including SHR (AT4G37650), BHLH96 (AT1G72210), GATA7 (AT4G36240) and WRKY12 (AT2G44745).

Most of the up-regulated TFs after C_4 manifestation belonged to C2H2 and bZIP families, and HY5 was part of this group. HY5 is a master regulator of transcription (Gangappa and Botto, 2016), a phloem-mediated shoot-to-root signal for lateral root formation, and thus the carbon-nitrogen balance adjustment in Arabidopsis (Burko *et al.*, 2020). HY5 mediates photomorphogenesis so that it is located downstream of Phytochrome B (phyB), the sensor of light and temperature (Legris *et al.*, 2016). Thus, in C_4 plants where shoots are exposed to high light intensity and temperature, and since the function of HY5 is conserved in many plants (Yamawaki *et al.*, 2011; Huai, Jing and Lin, 2020), HY5 can be an appropriate

candidate for synchronizing shoots and roots. Moreover, HY5 is one of the light-responsive TFs essential in inhibiting hypocotyl elongation during seedling (Oyama, Shimura and Okada, 1997). Therefore, HY5 is a shared regulator between several various pathways.

According to the TAIR database, the mRNA of 12 TFs annotated by PlantTFDB have cell-to-cell mobility (Table 2). We also predicted the probable cis-elements present in the promoter region of their orthologous in *A. thaliana*. More of the predicted cis-elements in the mobile TFs were light- and stress-responsive (Supplementary Table S4). It indicates that the expression and subsequent movement of these mobile TFs are influenced by abiotic stress, especially drought. One of them is WRKY40, and it has been revealed that ZmWRKY40 in *Zea mays* is a drought-responsive gene (Wang *et al.*, 2018). Several cis-regulatory elements were reported in the promoter region of ZmWRKY40, which contains abiotic stress elements such as ABRE, GARE, W-box, and MYB. There are also stress-related elements in the WRKY40 promoter in this study in which ABRE, GARE, and MYB are shared. In addition, MBS and TC-rich repeats were predicted as well. HAT22, which was up-regulated in hypocotyl B, is also involved in the abiotic stress control in Arabidopsis, where its mRNA level is raised under water deficit conditions (Huang *et al.*, 2008). HSFs play an essential role in responding to several abiotic stresses through the regulation of heat shock proteins (HSP) (Nishizawa-Yokoi *et al.*, 2011). It was previously reported that A1 subclass HSF is a master regulator of sensing stress and downstream HSP activation and affects the thermotolerance level. HSFA1e was more expressed in hypocotyl B, which is implicated in the tolerance to heat shock stress via transcriptional regulation of HsfA2 function (Nishizawa-Yokoi *et al.*, 2011). Besides, overexpression of maize ZmHsf06 in Arabidopsis, a member of subclass A1, leads to stronger drought-stress tolerance and growth advantages (H. Li *et al.*, 2015). Moreover, it has already been indicated that HSFB is a negative regulator in plants. HSFB2A is less expressed in hypocotyl B. ZmHsf08, a member of subclass B1, is down-regulated in

response to drought and salt in maize (Wang *et al.*, 2021). Besides, Promoter analysis in many genes affected by water deficit has already revealed that most of these are regulated by ABRE in their promoter region (Nakashima, Ito and Yamaguchi-Shinozaki, 2009).

Taken together, our data provide a valuable source for further functional genomic and genetic studies to identify master regulators underlying the coordination of developmental changes associated with functional C_4 photosynthesis. Also, our data fill the gap in previous studies which solely performed on the species that perform NADP-ME subtype of C4 after C3 photosynthesis in their life cycle and enabled comparative studies between different biochemical subtypes of C_4 photosynthesis.

FUNDING

A.M.B-M gratefully acknowledges the financial support from the Iran National Science Foundation (INSF) [funding reference number 95838484].

ACKNOWLEDGMENTS

We thank Stanislav Kopriva (University of Cologne) for critical reading of the manuscript. We also would like to thank Alexander Rudov and Hossein Akhani (University of Tehran) for their support during seed collection.

SUPPLEMENTARY MATERIALS

Supplementary Table S1. Summary of A) sequencing information B) De novo transcriptome assembly results by Trinity

Supplementary Table S2. The accession number of uploaded raw sequences to …

Supplementary Table S3. Active functional classes in the first leaves, hypocotyl A and hypocotyl B

Supplementary Table S4. Abundance (total mean TPM) of C_4-related proteins

Supplementary Table S5. Transcript abundance, statistics of differentially expressed genes and their annotation.

Supplementary Table S6. List of the unique and shared genes in comparison of DEGs of two developmental *H.mollissima*'s hypocotyls and identified genes related to the hypocotyl developments in flax (Roach and Deyholos, 2008) and hemp (Behr *et al.*, 2018) based on their assaigned Arabidopsis ID.

Supplementary Table S7. Functional analysis of the Cell signaling genes using Mapman

Supplementary Table S8. Differentially transcription factor genes between hypocotyl A and hypocotyl B using PlantTFDB v5.0

Supplementary Table S9. Cis-elements located the upstream of orthologous transcription factor genes with mobile mRNA in Arabidopsis

Supplementary Figure 1 Venn diagram analysis of DEGs of two developmental *H.mollissima*'s hypocotyls and identified genes related to the hypocotyl developments

in flax (Roach and Deyholos, 2008) and hemp (Behr *et al.*, 2018) based on their assaigned Arabidopsis ID.

REFERENCES:

Akhani, H. *et al.* (2009). Does Bienertia cycloptera with the single-cell system of C4 photosynthesis exhibit a seasonal pattern of δ13C values in nature similar to co-existing C4 Chenopodiaceae having the dual-cell (Kranz) system?. *Photosynthesis Research*, 99(1), pp. 23–36.

Argyros, R.D. *et al.* (2008). Type B response regulators of Arabidopsis play key roles in cytokinin signaling and plant development. *The Plant Cell*, 20(8), pp. 2102–2116.

Bartusch, K. and Melnyk, C.W. (2020). Insights into plant surgery: an overview of the multiple grafting techniques for Arabidopsis Thaliana. *Frontiers in Plant Science*, p. 2000.

Behr, M. *et al.* (2018). Insights into the molecular regulation of monolignol-derived product biosynthesis in the growing hemp hypocotyl. *BMC plant biology*, 18(1), pp. 1–18.

Bellstaedt, J. *et al.* (2019). A mobile auxin signal connects temperature sensing in cotyledons with growth responses in hypocotyls. *Plant Physiology*, 180(2), pp. 757–766.

Burko, Y. *et al.* (2020). Local HY5 activity mediates hypocotyl growth and shoot-to-root communication. *Plant communications*, 1(5), p. 100078.

Chen, X. *et al.* (2016). Shoot-to-root mobile transcription factor HY5 coordinates plant carbon and nitrogen acquisition. *Current Biology*, 26(5), pp. 640–646.

Chomczynski, P. and Sacchi, N. (1987). Single-step method of RNA isolation by acid guanidinium thiocyanate-phenol-chloroform extraction. *Analytical biochemistry*, 162(1), pp. 156–159.

Cui, H. (2021). Challenges and Approaches to Crop Improvement Through C3-to-C4 Engineering. *Frontiers in Plant Science*, p. 1851.

Dolan, L. (2001). Root patterning: SHORT ROOT on the move. *Current biology*, 11(23), pp. R983–R985.

Dubbe, D.R., Farquhar, G.D. and Raschke, K. (1978). Effect of abscisic acid on the gain of the feedback loop involving carbon dioxide and stomata. *Plant Physiology*, 62(3), pp. 413–417.

Fatima, Z. *et al.* (2018). Resource use efficiencies of C3 and C4 cereals under split nitrogen regimes. *Agronomy*, 8(5), p. 69.

Forde, B.G. (2002). Local and long-range signaling pathways regulating plant responses to nitrate. *Annual Review of Plant Biology*, 53(1), pp. 203–224.

Fukaki, H. and Tasaka, M. (2009). Hormone interactions during lateral root formation. *Plant molecular biology*, 69(4), pp. 437–449.

Gangappa, S.N. and Botto, J.F. (2016). The multifaceted roles of HY5 in plant growth and development. *Molecular plant*, 9(10), pp. 1353–1365.

Gerlich, S.C. *et al.* (2018). Sulfate metabolism in C4 Flaveria species is controlled by the root and connected to serine biosynthesis. *Plant physiology*, 178(2), pp. 565–582.

Gowik, U. *et al.* (2011). Evolution of C4 photosynthesis in the genus Flaveria: how many and which genes does it take to make C4?. *The Plant Cell*, 23(6), pp. 2087–2105.

Gowik, U. and Westhoff, P. (2011). The path from C3 to C4 photosynthesis. *Plant Physiology*, 155(1), pp. 56–63.

Grabherr, M.G. *et al.* (2011). Full-length transcriptome assembly from RNA-Seq data without a reference genome. *Nature biotechnology*, 29(7), pp. 644–652.

Haas, B. and Papanicolaou, A. (2016). TransDecoder (find coding regions within transcripts). *Google Scholar* [Preprint].

Hibberd, J.M. and Covshoff, S. (2010). The regulation of gene expression required for C4 photosynthesis. *Annual review of plant biology*, 61, pp. 181–207.

Hirner, A. *et al.* (2006). Arabidopsis LHT1 is a high-affinity transporter for cellular amino acid uptake in both root epidermis and leaf mesophyll. *The Plant Cell*, 18(8), pp. 1931–1946.

Huai, J., Jing, Y. and Lin, R. (2020). Functional analysis of ZmCOP1 and ZmHY5 reveals conserved light signaling mechanism in maize and Arabidopsis. *Physiologia Plantarum*, 169(3), pp. 369–379.

Huang, C.-F. *et al.* (2017). Elevated auxin biosynthesis and transport underlie high vein density in C4 leaves. *Proceedings of the National Academy of Sciences*, 114(33), pp. E6884–E6891.

Huang, D. *et al.* (2008). The relationship of drought-related gene expression in Arabidopsis thaliana to hormonal and environmental factors. *Journal of experimental Botany*, 59(11), pp. 2991–3007.

Huxman, T.E. and Monson, R.K. (2003). Stomatal responses of C3, C3□C4 and C4Flaveria species to light and intercellular CO2 concentration: implications for the evolution of stomatal behaviour. *Plant, Cell & Environment*, 26(2), pp. 313–322.

Jobe, T.O. *et al.* (2020). Ensuring nutritious food under elevated CO2 conditions: A case for improved C4 crops. *Frontiers in Plant Science*, 11, p. 1267.

Kang, J. *et al.* (2010). PDR-type ABC transporter mediates cellular uptake of the phytohormone abscisic acid. *Proceedings of the National Academy of sciences*, 107(5), pp. 2355–2360.

Kang, J. *et al.* (2015). Abscisic acid transporters cooperate to control seed germination. *Nature communications*, 6(1), pp. 1–10.

Kiba, T. *et al.* (2011). Hormonal control of nitrogen acquisition: roles of auxin, abscisic acid, and cytokinin. *Journal of experimental botany*, 62(4), pp. 1399–1409.

Ko, D. and Helariutta, Y. (2017). Shoot–root communication in flowering plants. *Current Biology*, 27(17), pp. R973–R978.

Koenig, A.M. and Hoffmann-Benning, S. (2020). The interplay of phloem-mobile signals in plant development and stress response. *Bioscience Reports*, 40(10).

Kurakawa, T. *et al.* (2007). Direct control of shoot meristem activity by a cytokinin-activating enzyme. *Nature*, 445(7128), pp. 652–655.

Kuromori, T., Seo, M. and Shinozaki, K. (2018). ABA transport and plant water stress responses. *Trends in plant science*, 23(6), pp. 513–522.

Lacombe, B. and Achard, P. (2016). Long-distance transport of phytohormones through the plant vascular system. *Current opinion in plant biology*, 34, pp. 1–8.

Lauterbach, M., Billakurthi, K., *et al.* (2017). C3 cotyledons are followed by C4 leaves: intra-individual transcriptome analysis of Salsola soda (Chenopodiaceae). *Journal of experimental botany*, 68(2), pp. 161–176.

Lauterbach, M., Schmidt, H., *et al.* (2017). De novo transcriptome assembly and comparison of C3, C3-C4, and C4 species of tribe Salsoleae (Chenopodiaceae). *Frontiers in plant science*, 8, p. 1939.

Legris, M. *et al*. (2016). Phytochrome B integrates light and temperature signals in Arabidopsis. *Science*, 354(6314), pp. 897–900.

Lescot, M. *et al*. (2002). PlantCARE, a database of plant cis-acting regulatory elements and a portal to tools for in silico analysis of promoter sequences. *Nucleic acids research*, 30(1), pp. 325–327.

Li, B. and Dewey, C.N. (2011). RSEM: accurate transcript quantification from RNA-Seq data with or without a reference genome. *BMC bioinformatics*, 12(1), pp. 1–16.

Li, H. *et al*. (2015). Expression of maize heat shock transcription factor gene ZmHsf06 enhances the thermotolerance and drought-stress tolerance of transgenic Arabidopsis. *Functional Plant Biology*, 42(11), pp. 1080–1091.

Li, Y. *et al*. (2015). Developmental genetic mechanisms of C4 syndrome based on transcriptome analysis of C3 cotyledons and C4 assimilating shoots in Haloxylon ammodendron. *PLoS One*, 10(2), p. e0117175.

Liu, C.-J., Zhao, Y. and Zhang, K. (2019). Cytokinin transporters: multisite players in cytokinin homeostasis and signal distribution. *Frontiers in Plant Science*, p. 693.

Lohse, M. *et al*. (2014) *M ercator: a fast and simple web server for genome scale functional annotation of plant sequence data*. Wiley Online Library.

Marshall, E., Costa, L.M. and Gutierrez-Marcos, J. (2011). Cysteine-rich peptides (CRPs) mediate diverse aspects of cell–cell communication in plant reproduction and development. *Journal of experimental botany*, 62(5), pp. 1677–1686.

McKown, A.D. and Dengler, N.G. (2007). Key innovations in the evolution of Kranz anatomy and C4 vein pattern in Flaveria (Asteraceae). *American journal of botany*, 94(3), pp. 382–399.

Morse, M., Pironcheva, G. and Gehring, C. (2004). AtPNP□A is a systemically mobile natriuretic peptide immunoanalogue with a role in Arabidopsis thaliana cell volume regulation. *FEBS letters*, 556(1–3), pp. 99–103.

Nakashima, K., Ito, Y. and Yamaguchi-Shinozaki, K. (2009). Transcriptional regulatory networks in response to abiotic stresses in Arabidopsis and grasses. *Plant physiology*, 149(1), pp. 88–95.

Nishizawa-Yokoi, A. *et al.* (2011). HsfA1d and HsfA1e involved in the transcriptional regulation of HsfA2 function as key regulators for the Hsf signaling network in response to environmental stress. *Plant and Cell Physiology*, 52(5), pp. 933–945.

Ohkubo, Y. *et al*. (2017). Shoot-to-root mobile polypeptides involved in systemic regulation of nitrogen acquisition. *Nature plants*, 3(4), pp. 1–6.

Okamoto, S., Tabata, R. and Matsubayashi, Y. (2016). Long-distance peptide signaling essential for nutrient homeostasis in plants. *Current opinion in plant biology*, 34, pp. 35–40.

Oyama, T., Shimura, Y. and Okada, K. (1997). The Arabidopsis HY5 gene encodes a bZIP protein that regulates stimulus-induced development of root and hypocotyl. *Genes & development*, 11(22), pp. 2983–2995.

Rao, X. and Dixon, R.A. (2016). The differences between NAD-ME and NADP-ME subtypes of C4 photosynthesis: more than decarboxylating enzymes. *Frontiers in plant*

science, 7, p. 1525.

Reyna-Llorens, I. and Hibberd, J.M. (2017). Recruitment of pre-existing networks during the evolution of C4 photosynthesis. *Philosophical Transactions of the Royal Society B: Biological Sciences*, 372(1730), p. 20160386.

Roach, M.J. and Deyholos, M.K. (2008). Microarray analysis of developing flax hypocotyls identifies novel transcripts correlated with specific stages of phloem fibre differentiation. *Annals of botany*, 102(3), pp. 317–330.

Robinson, M.D., McCarthy, D.J. and Smyth, G.K. (2010). edgeR: a Bioconductor package for differential expression analysis of digital gene expression data. *Bioinformatics*, 26(1), pp. 139–140.

Rudov, A. *et al.* (2020). A review of C4 plants in southwest Asia: An ecological, geographical and taxonomical analysis of a region with high diversity of C4 eudicots. *Frontiers in plant science*, 11, p. 1374.

Ruffel, S. *et al.* (2008). Systemic signaling of the plant nitrogen status triggers specific transcriptome responses depending on the nitrogen source in Medicago truncatula. *Plant physiology*, 146(4), pp. 2020–2035.

Sadanandom, A. *et al.* (2012). The ubiquitin–proteasome system: central modifier of plant signalling. *New Phytologist*, 196(1), pp. 13–28.

Sage, R.F. (2004). The evolution of C4 photosynthesis. *New phytologist*, 161(2), pp. 341–370.

Sampaio Filho, I. de J. *et al.* (2018). Below versus above ground plant sources of abscisic acid (ABA) at the heart of tropical forest response to warming. *International journal of molecular sciences*, 19(7), p. 2023.

Sauer, M. and Kleine-Vehn, J. (2019). PIN-FORMED and PIN-LIKES auxin transport facilitators. *Development*, 146(15), p. dev168088.

Schwacke, R. *et al.* (2019). MapMan4: a refined protein classification and annotation framework applicable to multi-omics data analysis. *Molecular plant*, 12(6), pp. 879–892.

Shabala, S. *et al.* (2015). Root-to-shoot signalling: integration of diverse molecules, pathways and functions. *Functional Plant Biology*, 43(2), pp. 87–104.

Shao, H., Wang, H. and Tang, X. (2015). NAC transcription factors in plant multiple abiotic stress responses: progress and prospects. *Frontiers in plant science*, 6, p. 902.

Siadjeu, C., Lauterbach, M. and Kadereit, G. (2021). Insights into regulation of C2 and C4 photosynthesis in Amaranthaceae/Chenopodiaceae using RNA-Seq. *International journal of molecular sciences*, 22(22), p. 12120.

Slewinski, T.L. *et al.* (2012). Scarecrow plays a role in establishing Kranz anatomy in maize leaves. *Plant and Cell Physiology*, 53(12), pp. 2030–2037.

Slewinski, T.L. (2013). Using evolution as a guide to engineer Kranz-type C4 photosynthesis. *Frontiers in plant science*, 4, p. 212.

Smets, R. *et al.* (2005). Cytokinin-induced hypocotyl elongation in light-grown Arabidopsis plants with inhibited ethylene action or indole-3-acetic acid transport. *Planta*, 221(1), pp. 39–47.

Sun, J. and Zheng, N. (2015). Molecular mechanism underlying the plant NRT1. 1 dual-affinity nitrate transporter. *Frontiers in Physiology*, 6, p. 386.

Tabata, R. *et al.* (2014). Perception of root-derived peptides by shoot LRR-RKs mediates systemic N-demand signaling. *Science*, 346(6207), pp. 343–346.

Tian, Q. *et al.* (2008). Inhibition of maize root growth by high nitrate supply is correlated with reduced IAA levels in roots. *Journal of plant physiology*, 165(9), pp. 942–951.

To, J.P.C. *et al.* (2004). Type-A Arabidopsis response regulators are partially redundant negative regulators of cytokinin signaling. *The Plant Cell*, 16(3), pp. 658–671.

Ueno, O. (1998). Induction of Kranz anatomy and C4-like biochemical characteristics in a submerged amphibious plant by abscisic acid. *The Plant Cell*, 10(4), pp. 571–583.

Usadel, B. *et al.* (2006). PageMan: an interactive ontology tool to generate, display, and annotate overview graphs for profiling experiments. *BMC bioinformatics*, 7(1), pp. 1–8.

Vogan, P.J. and Sage, R.F. (2011). Water□use efficiency and nitrogen□use efficiency of C3□C4 intermediate species of Flaveria Juss.(Asteraceae). *Plant, cell & environment*, 34(9), pp. 1415–1430.

Wang, C.-T. *et al.* (2018). The maize WRKY transcription factor ZmWRKY40 confers drought resistance in transgenic Arabidopsis. *International journal of molecular sciences*, 19(9), p. 2580.

Wang, J. *et al.* (2021). A Novel Heat Shock Transcription Factor (ZmHsf08) Negatively Regulates Salt and Drought Stress Responses in Maize. *International journal of molecular sciences*, 22(21), p. 11922.

Wang, L. *et al.* (2014). Comparative analyses of C4 and C3 photosynthesis in developing leaves of maize and rice. *Nature biotechnology*, 32(11), pp. 1158–1165.

Wang, P., Vlad, D. and Langdale, J.A. (2016). Finding the genes to build C4 rice. *Current Opinion in Plant Biology*, 31, pp. 44–50.

Wang, W. *et al.* (2020). NRT1. 1s in plants: functions beyond nitrate transport. *Journal of Experimental Botany*, 71(15), pp. 4373–4379.

Wilkinson, S. and Davies, W.J. (2002). ABA□based chemical signalling: the co□ordination of responses to stress in plants. *Plant, cell & environment*, 25(2), pp. 195–210.

Yamawaki, S. *et al.* (2011). Functional characterization of HY5 homolog genes involved in early light-signaling in Physcomitrella patens. *Bioscience, biotechnology, and biochemistry*, 75(8), pp. 1533–1539.

Zhang, H. *et al.* (2014). A DTX/MATE-type transporter facilitates abscisic acid efflux and modulates ABA sensitivity and drought tolerance in Arabidopsis. *Molecular plant*, 7(10), pp. 1522–1532.

Zhao, H. *et al.* (2017). The Arabidopsis thaliana nuclear factor Y transcription factors. *Frontiers in plant science*, 7, p. 2045.

CAPTION of Table:

Table 1. List of differentially expressed transcription factors between hypocotyl A and hypocotyl B with mobile mRNAs based on TAIR database (https://www.arabidopsis.org/)

Arabidopsis ID	Transcription factor name	Transcription factor family	Log_2FC	FDR
AT3G10500	NAC053	NAC	10/19	7/19E-05
AT1G09770	CDC5	MYB_related	9/78	0/001280562
AT3G02990	HSFA1E	HSF	3/16	2/80E-05
AT1G69490	NAP	NAC	2/43	6/08E-06
AT1G21450	SCL1	GRAS	2/03	7/52E-10
AT1G80840	WRKY40	WRKY	1/62	2/32E-12
AT4G37790	HAT22	HD-ZIP	1/55	8/04E-06
AT5G47390	MYBH	MYB_related	1/52	1/21E-09
AT5G62020	HSFB2A	HSF	-1/84	2/75E-06
AT5G60690	REV	HD-ZIP	-3/12	0/030388143
AT5G59570	BOA	G2-like	-4/08	0/013424766
AT1G01720	ATAF1	NAC	-11/88	2/42E-21

CAPTION of Figures:

Figure 1. Sampled tissues from *H. mollissima* in the current study

Figure 2. PCA analysis which explains 91.09% of the total variation

Figure 3. Active functional classes of each sample according to all percentage of all transcripts belonged to Mapman categories

Figure 4. Relative transcript abundance of C_4 cycle proteins: most C4 proteins are more expressed in leaves than in hypocotyls. Beta-carbonic anhydrase (BCA3), PEP carboxylase1 (PEPC1), pyruvate orthophosphate dikinase (PPdK), aspartate aminotransferase (Asp-AT), alanine aminotransferase (Ala-AT), NAD-dependent malic enzyme (NAD-ME), NADP-dependent malic enzyme (NADP-ME), Triosephosphate translocator (TPT), Pyrophosphatase (PPase6), pyruvate orthophosphate dikinase related protein1 (PPdK-RP1), PEP/phosphate translocator (PPT2), Bile acid:sodium symporter family protein (BASS4), Bile acid:sodium symporter family protein (BASS2), Adenosine monophosphate kinase (AMK2), Dicarboxylate translocator1 (Dit1), phosphoenolpyruvate carboxykinase (PEPC-K)

Figure 5. UpSet plot: showing the number of unique and shared differentially expressed genes of *H.mollissima* between each binary comparison of samples

Figure 6. Overrepresentation analysis of up-and down-regulated genes in pairwise comparison of hypocotyl B vs. hypocotyl A within functional gene classes defined by MapMan bins (MapMan, v3.6, available online at https://www.plabipd.de/portal/mercator4) in Pageman software. 'Fisher's exact test followed by the Benjamini Hochberg correction and cut-off value one was used for functional enrichment of differentially expressed genes between three binary comparisons

Figure 7. "Cell signaling" using MapMan. Visualization of transcriptional changes in genes involved in the various signaling pathways (FDR<0.05, log2FC>1.5 <-1.5) at hypocotyl B Vs. hypocotyl A

Figure 8. Relative transcript abundance of transcripts associated with (A) CRP peptide activities (B) NCRP peptide activities

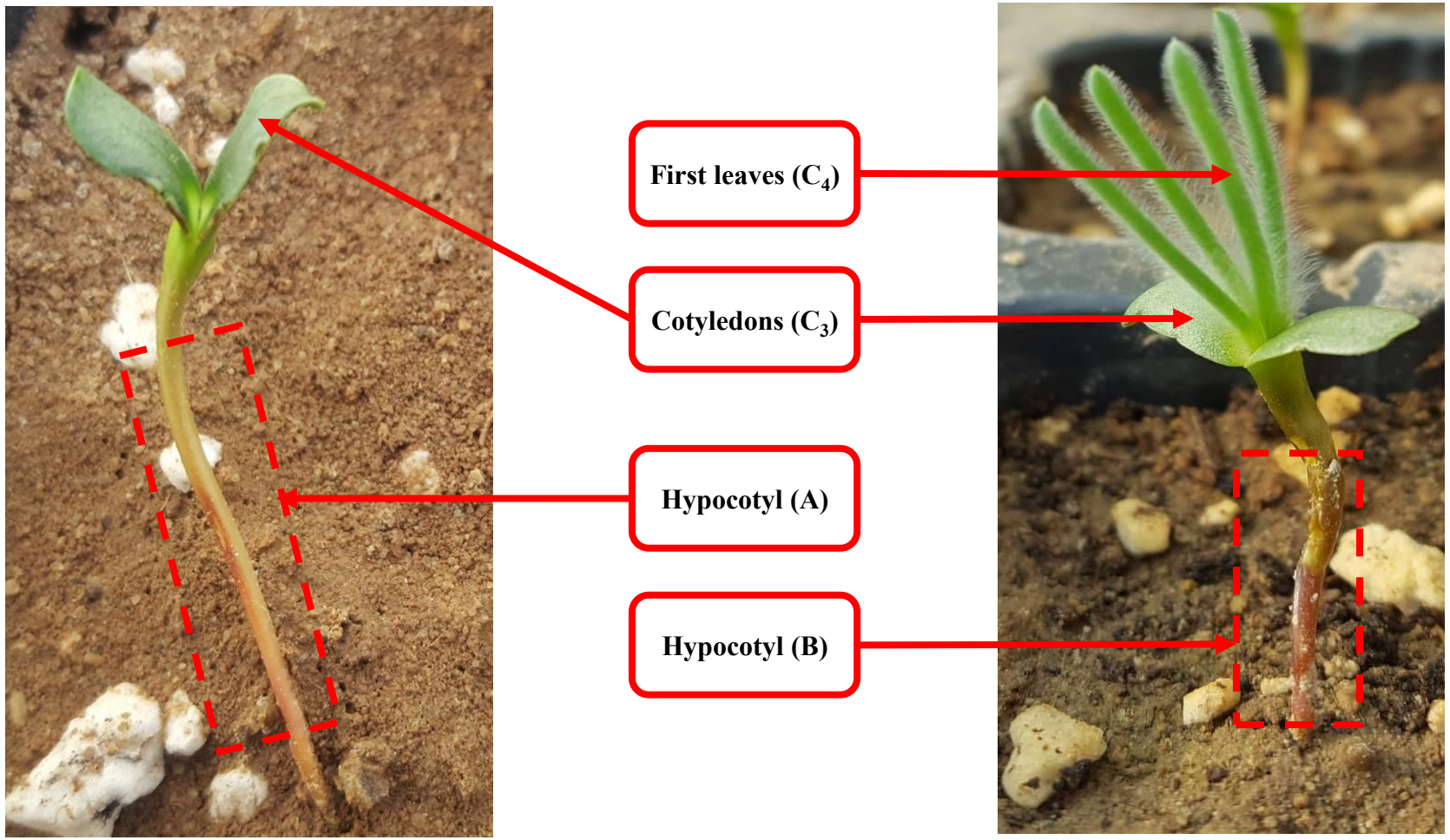
First leaves (C_4)
Cotyledons (C_3)
Hypocotyl (A)
Hypocotyl (B)

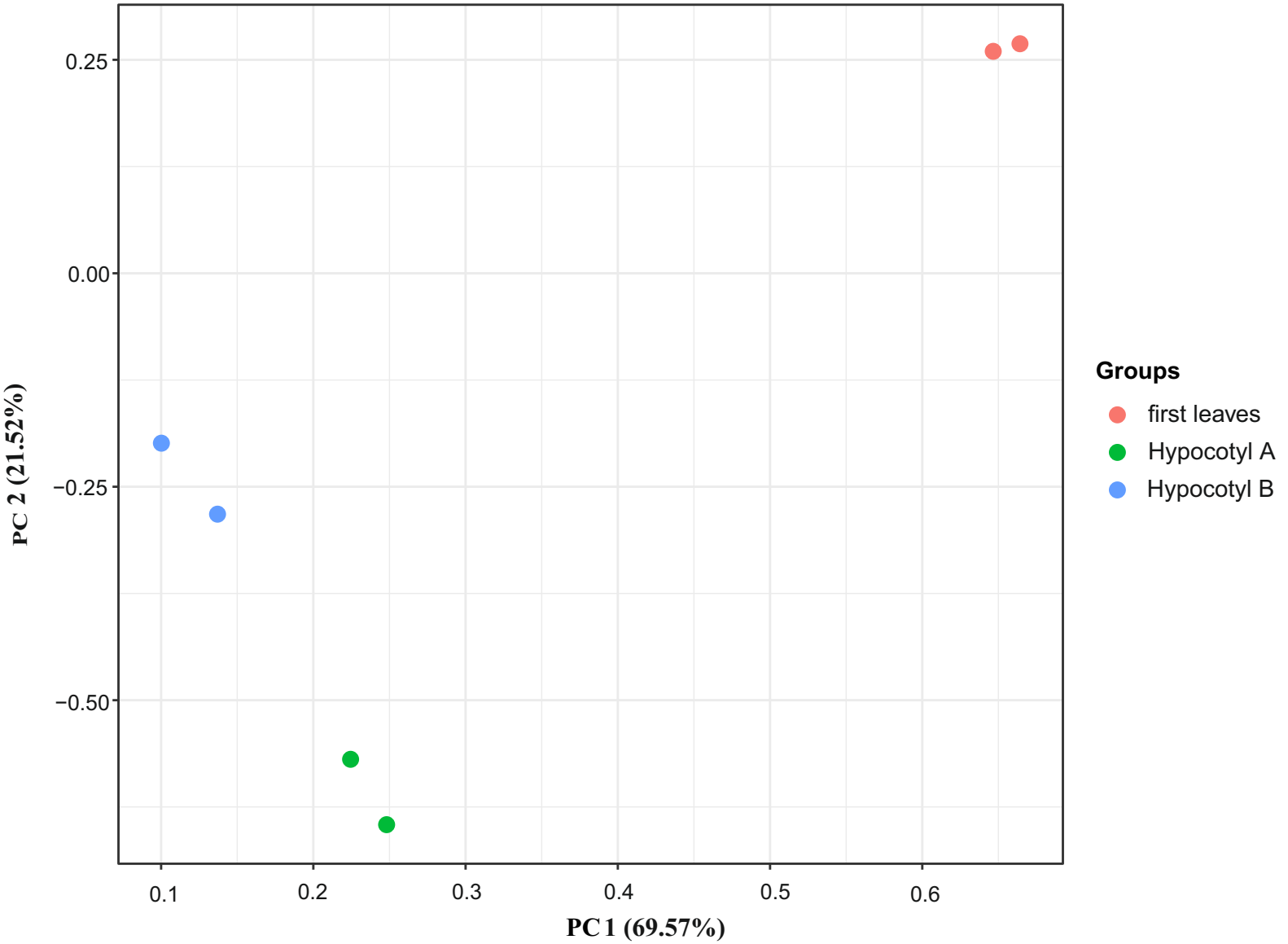
0.25
0.00
−0.25
−0.50
PC 2 (21.52%)
0.1
0.2
0.3
0.4
0.5
0.6
PC 1 (69.57%)
Groups
first leaves
Hypocotyl A
Hypocotyl B

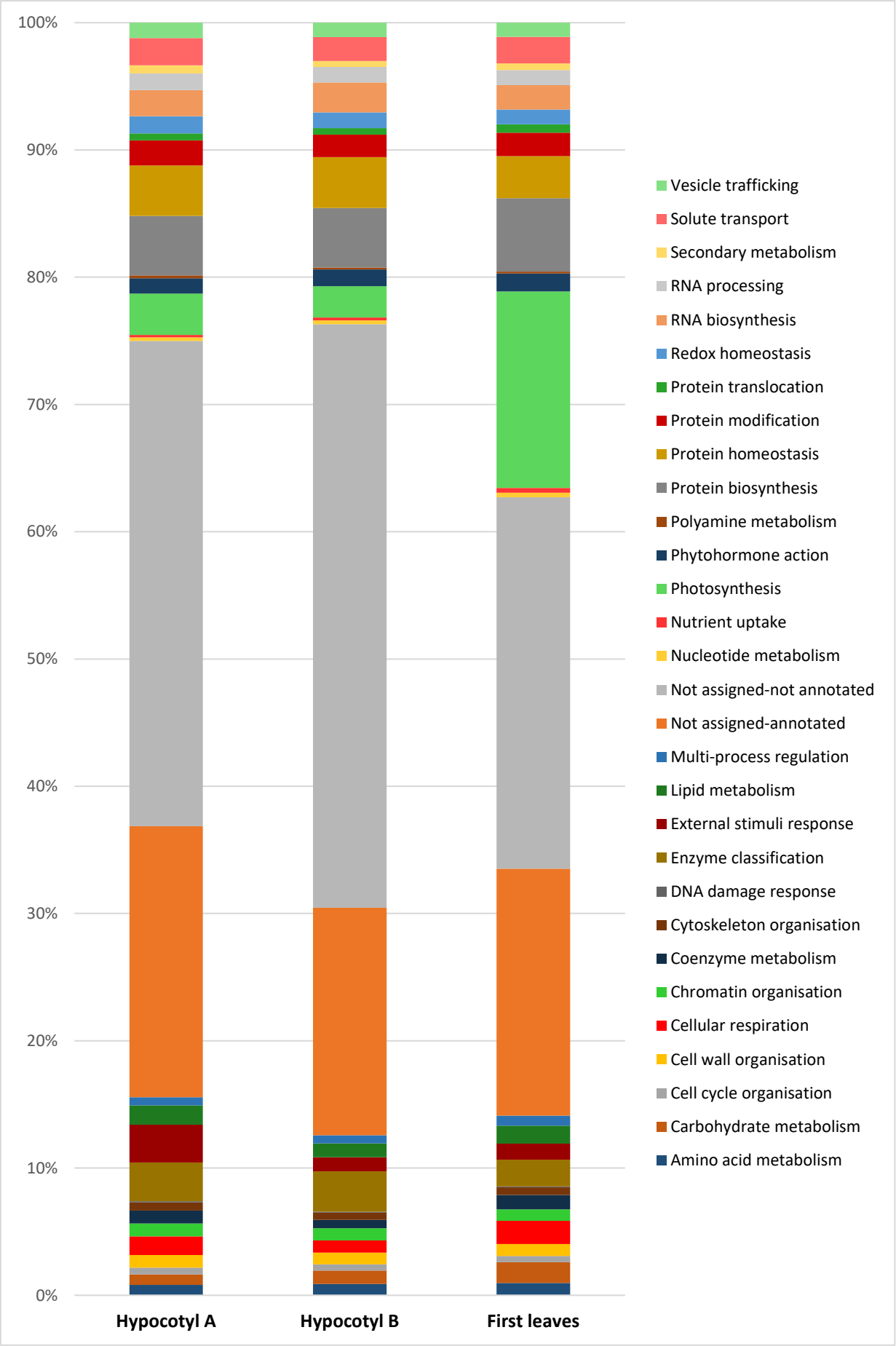
100%
90%
80%
70%
60%
50%
40%
30%
20%
10%
0%
Hypocotyl A
Hypocotyl B
First leaves
Vesicle trafficking
Solute transport
Secondary metabolism
RNA processing
RNA biosynthesis
Redox homeostasis
Protein translocation
Protein modification
Protein homeostasis
Protein biosynthesis
Polyamine metabolism
Phytohormone action
Photosynthesis
Nutrient uptake
Nucleotide metabolism
Not assigned-not annotated
Not assigned-annotated
Multi-process regulation
Lipid metabolism
External stimuli response
Enzyme classification
DNA damage response
Cytoskeleton organisation
Coenzyme metabolism
Chromatin organisation
Cellular respiration
Cell wall organisation
Cell cycle organisation
Carbohydrate metabolism
Amino acid metabolism

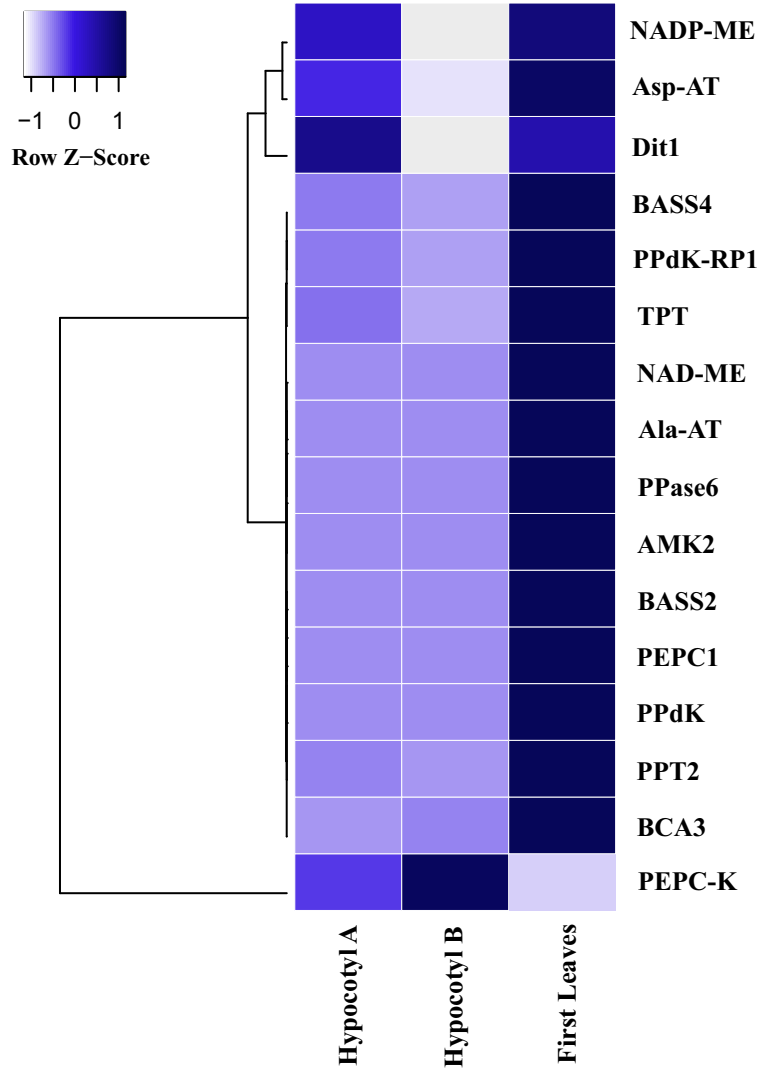
−1 0 1
Row Z−Score
NADP-ME
Asp-AT
Dit1
BASS4
PPdK-RP1
TPT
NAD-ME
Ala-AT
PPase6
AMK2
BASS2
PEPC1
PPdK
PPT2
BCA3
PEPC-K
Hypocotyl A
Hypocotyl B
First Leaves

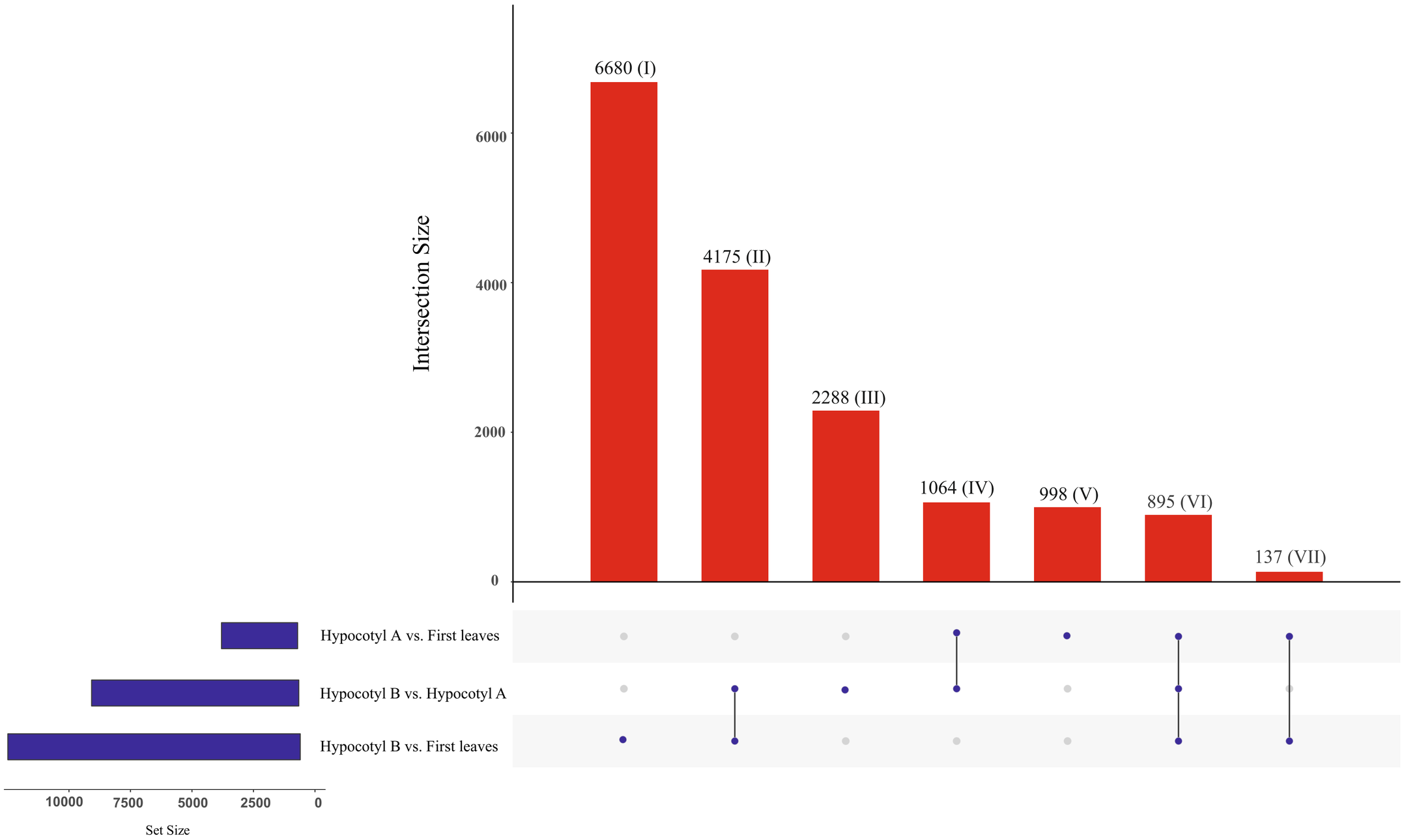
Intersection Size
6000
4000
2000
0
6680 (I)
4175 (II)
2288 (III)
1064 (IV)
998 (V)
895 (VI)
137 (VII)
Hypocotyl A vs. First leaves
Hypocotyl B vs. Hypocotyl A
Hypocotyl B vs. First leaves
10000
7500
5000
2500
0
Set Size

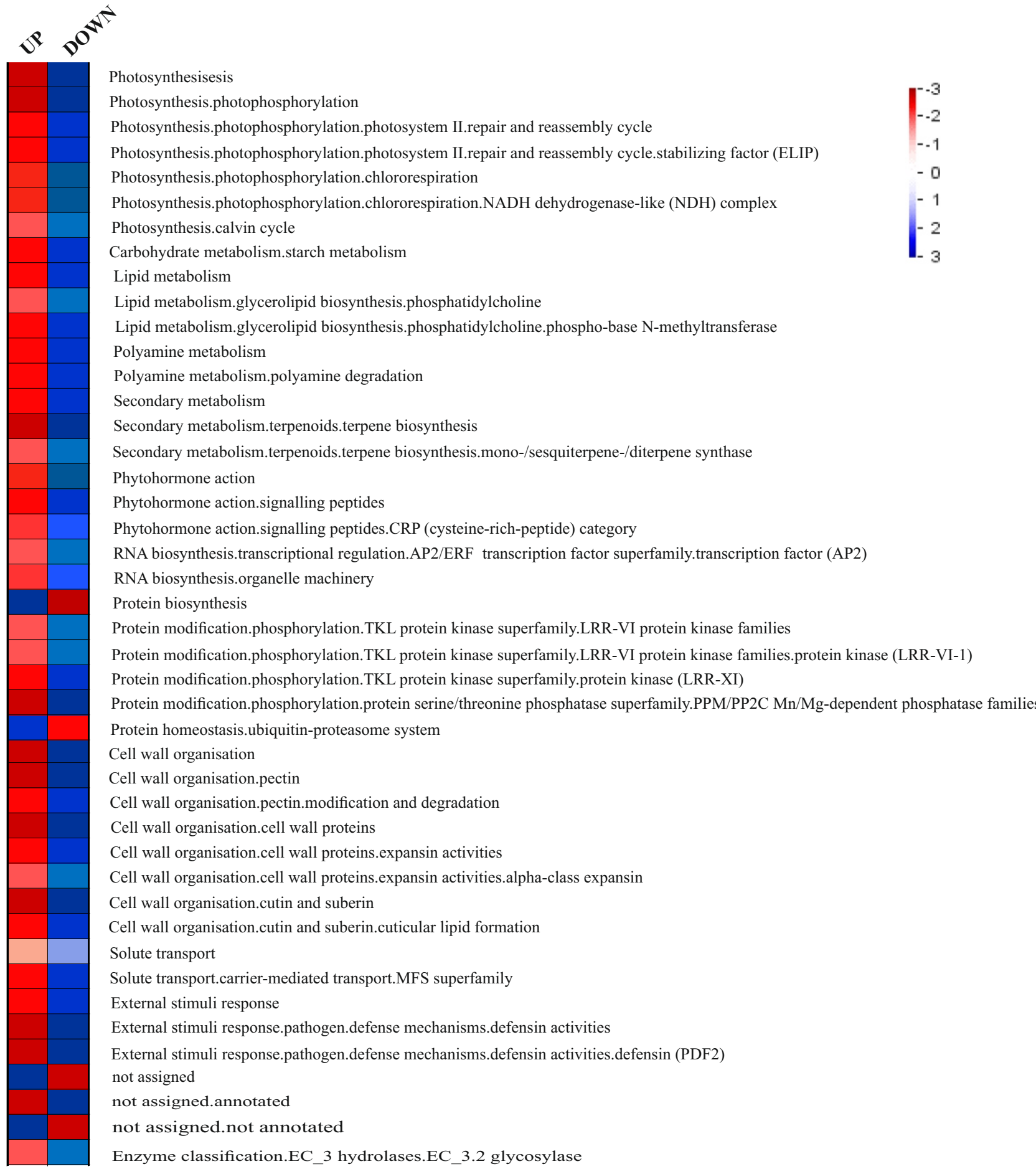
UP
DOWN
Photosynthesisesis
Photosynthesis.photophosphorylation
Photosynthesis.photophosphorylation.photosystem II.repair and reassembly cycle
Photosynthesis.photophosphorylation.photosystem II.repair and reassembly cycle.stabilizing factor (ELIP)
Photosynthesis.photophosphorylation.chlororespiration
Photosynthesis.photophosphorylation.chlororespiration.NADH dehydrogenase-like (NDH) complex
Photosynthesis.calvin cycle
Carbohydrate metabolism.starch metabolism
Lipid metabolism
Lipid metabolism.glycerolipid biosynthesis.phosphatidylcholine
Lipid metabolism.glycerolipid biosynthesis.phosphatidylcholine.phospho-base N-methyltransferase
Polyamine metabolism
Polyamine metabolism.polyamine degradation
Secondary metabolism
Secondary metabolism.terpenoids.terpene biosynthesis
Secondary metabolism.terpenoids.terpene biosynthesis.mono-/sesquiterpene-/diterpene synthase
Phytohormone action
Phytohormone action.signalling peptides
Phytohormone action.signalling peptides.CRP (cysteine-rich-peptide) category
RNA biosynthesis.transcriptional regulation.AP2/ERF transcription factor superfamily.transcription factor (AP2)
RNA biosynthesis.organelle machinery
Protein biosynthesis
Protein modification.phosphorylation.TKL protein kinase superfamily.LRR-VI protein kinase families
Protein modification.phosphorylation.TKL protein kinase superfamily.LRR-VI protein kinase families.protein kinase (LRR-VI-1)
Protein modification.phosphorylation.TKL protein kinase superfamily.protein kinase (LRR-XI)
Protein modification.phosphorylation.protein serine/threonine phosphatase superfamily.PPM/PP2C Mn/Mg-dependent phosphatase families
Protein homeostasis.ubiquitin-proteasome system
Cell wall organisation
Cell wall organisation.pectin
Cell wall organisation.pectin.modification and degradation
Cell wall organisation.cell wall proteins
Cell wall organisation.cell wall proteins.expansin activities
Cell wall organisation.cell wall proteins.expansin activities.alpha-class expansin
Cell wall organisation.cutin and suberin
Cell wall organisation.cutin and suberin.cuticular lipid formation
Solute transport
Solute transport.carrier-mediated transport.MFS superfamily
External stimuli response
External stimuli response.pathogen.defense mechanisms.defensin activities
External stimuli response.pathogen.defense mechanisms.defensin activities.defensin (PDF2)
not assigned
not assigned.annotated
not assigned.not annotated
Enzyme classification.EC_3 hydrolases.EC_3.2 glycosylase
-3
-2
-1
0
1
2
3

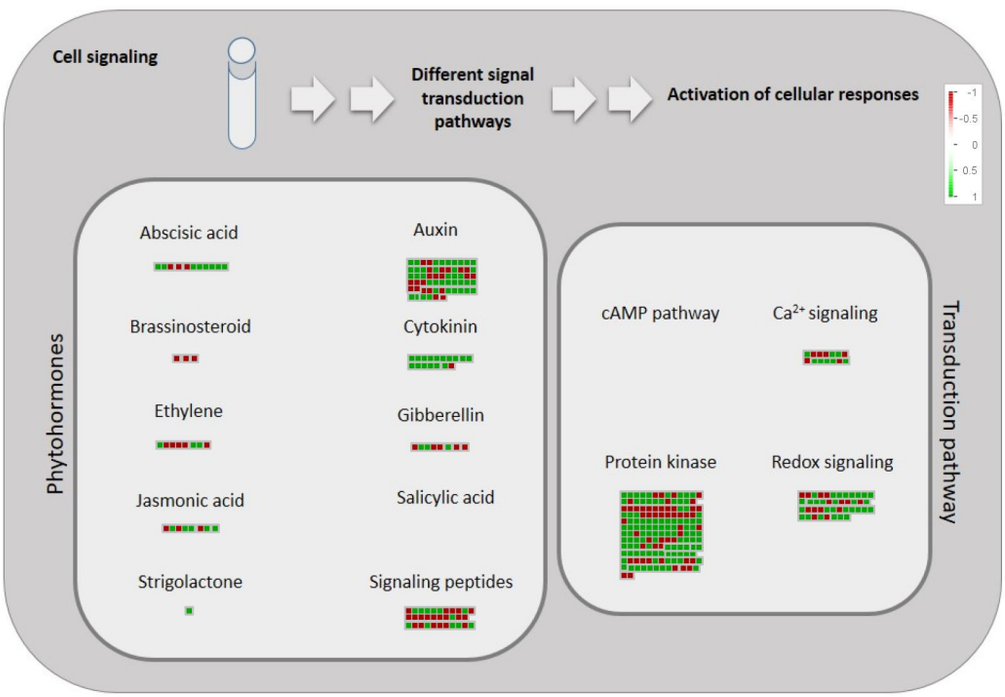

Cell signaling2.jpg
mapping: Job3638.results.txt
mapped: 8459 of 8084 data points
visible: 361 data points
data: Unique BA-New Mapman.xls

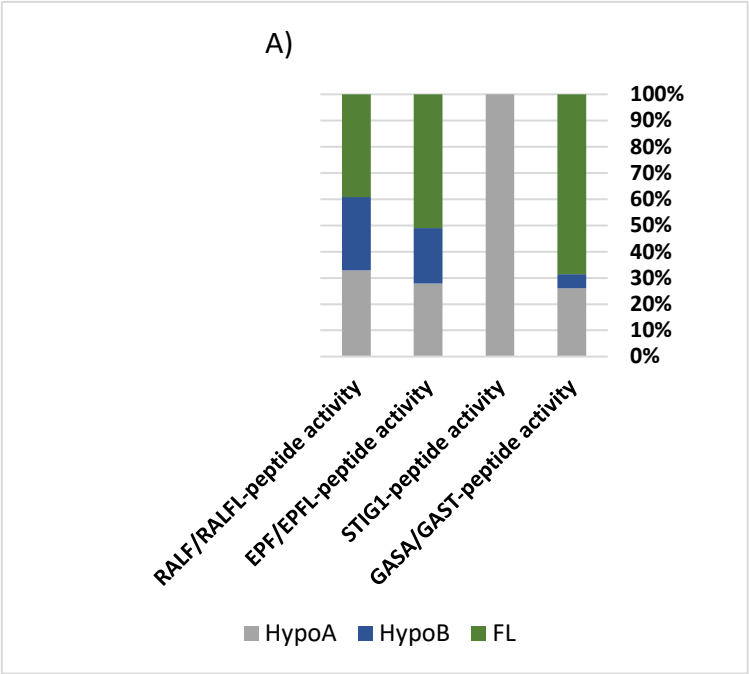
A)
100%
90%
80%
70%
60%
50%
40%
30%
20%
10%
0%
RALF/RALFL-peptide activity
EPF/EPFL-peptide activity
STIG1-peptide activity
GASA/GAST-peptide activity
HypoA
HypoB
FL

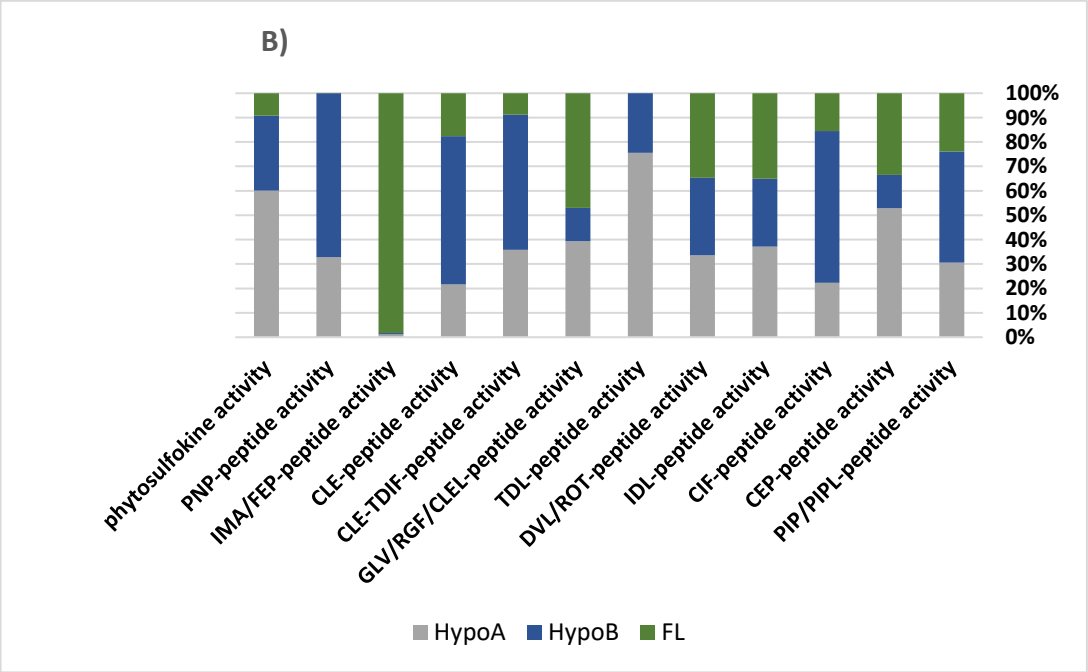
B)
100%
90%
80%
70%
60%
50%
40%
30%
20%
10%
0%
phytosulfokine activity
PNP-peptide activity
IMA/FEP-peptide activity
CLE-peptide activity
CLE-TDIF-peptide activity
GLV/RGF/CLEL-peptide activity
TDL-peptide activity
DVL/ROT-peptide activity
IDL-peptide activity
CIF-peptide activity
CEP-peptide activity
PIP/PIPL-peptide activity
HypoA
HypoB
FL